An Analytical Model of Temperature in Microprocessors

Pierre Michaud, Yiannakis Sazeides, André Seznec, Theofanis Constantinou, Damien Fetis

INRIA

INSTITUT NATIONAL DE RECHERCHE EN INFORMATIQUE ET EN AUTOMATIQUE

An Analytical Model of Temperature in Microprocessors

Pierre Michaud , Yiannakis Sazeides , André Seznec , Theofanis Constantinou ,

Damien Fetis

N°5744

Novembre 2005

Systèmes communicants

ISSN 0249-6399 ISRN INRIA/RR--5744--FR+ENG

An Analytical Model of Temperature in Microprocessors

Pierre Michaud [*] , Yiannakis Sazeides [†] , André Seznec [‡] , Theofanis Constantinou [§] , Damien Fetis [¶]

Systèmes communicants
Projet CAPS

Rapport de recherche n ° 5744 — Novembre 2005 — 32 pages

Abstract: Temperature has become an important design constraint for high-performance microprocessors. Research on temperature-constrained microarchitecture requires an efficient modeling of temperature. We propose an analytical model of temperature, based on solving a boundary-value problem of heat conduction. The model gives steady-state and transient temperature at any point on the dissipating plane, assuming rectangle-shaped surface sources. The model can be used to reason about temperature. It can also be implemented in a performance/power microarchitecture simulator. We provide two examples illustrating these uses.

Key-words: Microprocessor temperature, analytical model, steady state, transient, principle of superposition, point source, rectangle source, method of images

(Résumé : tsvp)

[*] pmichaud@irisa.fr
[†] yanos@cs.ucy.ac.cy
[‡] seznec@irisa.fr
[§] theofanis@cs.ucy.ac.cy
[¶] dfetis@irisa.fr

Unité de recherche INRIA Rennes
IRISA, Campus universitaire de Beaulieu, 35042 RENNES Cedex (France)
Téléphone : 02 99 84 71 00 - International : +33 2 99 84 71 00
Télécopie : 02 99 84 71 71 - International : +33 2 99 84 71 71

Un modèle analytique de la température des microprocesseurs

Résumé : La température est une contrainte importante sur les processeurs haute-performance récents. La recherche en microarchitecture, dans ce contexte, nécessite une modélisation efficace de la température. Nous proposons un modèle analytique de la température basé sur une solution de l'équation de la chaleur avec conditions aux limites. Le modèle donne la température en régime permanent et en régime transitoire en tout point sur la surface dissipante, en supposant des sources de chaleur surfaciques et de forme rectangulaire. Le modèle peut être utilisé pour raisonner sur la température. Il peut aussi être intégré dans un simulateur de microarchitecture. Nous présentons deux exemples illustrant ces utilisations.

Mots-clé : Température des microprocesseurs, modèle analytique, régime permanent, transitoire, principe de superposition, source ponctuelle, source rectangulaire, méthode des images

1 Introduction

Temperature has become an important design constraint for high-performance microprocessors [10, 8, 22]. The temperature problem results mainly from circuit miniaturization, which leads to increased power densities. Recently, temperature-aware microarchitecture has been central to many studies [17, 27, 11, 4, 6, 23, 26, 16]. These studies show that microarchitectural decisions may have an impact on temperature. Most temperature studies in the microarchitecture community model temperature with thermal RC networks.

The goal of this report is to provide an alternative tool, based on analytical modeling of heat conduction. Formulas in this report are primarily intended to be used as an analysis tool for understanding thermal phenomena in microprocessors. Some of these formulas can also be implemented in a performance/power microarchitecture simulator, as illustrated in Section 9.2.

This report is organized as follows. Section 2 describes our physical model. Section 3 discusses the principle of superposition, which we use extensively in the rest of the study. In Section 4, we give a detailed derivation of the solution of the heat equation for a point source dissipating a constant power. We show in Section 5 that this basic solution can be integrated to obtain the temperature generated by sources of various shapes. Solutions in Section 4 and 5 are given in the form of Laplace-transformed temperature. We show in Section 6 how to obtain the time-varying and steady-state temperature from the Laplace-transformed temperature. The base model described in Sections 2 to 6 assumes an infinite heat sink width. We show in Section 7 that the heat sink width can be taken into account by the method of images. Section 8 focuses on the temperature response to a periodic power. Finally, Section 9 provides two examples for the purpose of illustration.

Notations. Notations used in this study respect the following rules : t represents time, $w = T - T_{amb}$ represents relative temperature (T_{amb} being the ambient temperature, which is assumed to be uniform and constant), and q represents power density (or heat flux) in W/m^2. Notation $\overline{p}(s)$ is for the Laplace transform $\mathcal{L}\{p(t)\}$ of any function $p(t)$ of time.

2 A 2-layer model

We model the physical system as two layers of different materials, as depicted in Figure 1. The two layers are parallel to the (x, y) plane and perpendicular to the z direction. Layer 1 corresponds to $z \in [0, z_1]$ and represents the silicon die. Layer 2 corresponds to $z \in [z_1, z_2]$ and represents the heat sink base plate, which we assume is made of copper for good heat spreading.

We assume that the layers are infinite in the x and y directions (we show in Section 7 that the impact of a limited heat sink width can be taken into account by the method of images).

There is a thermal conductance h_1 between layers 1 and 2, and a thermal conductance h_2 between layer 2 and the ambient medium. Conductance h_1 represents the interface

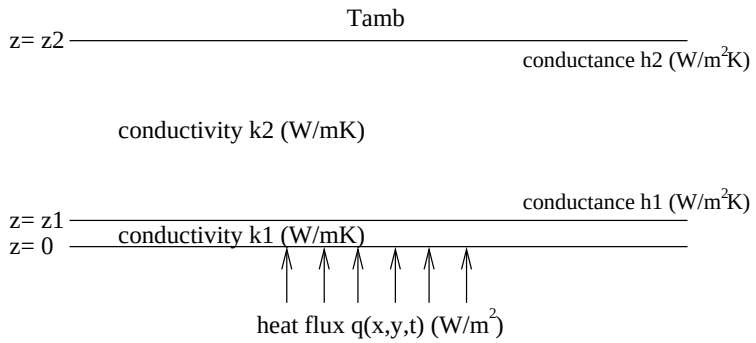

Figure 1: *A 2-layer model.*

locus	boundary condition
$z = 0$	$q(x,y,t) = -k_1 \frac{\partial T_1}{\partial z}$
$z = z_1$	$-k_1 \frac{\partial T_1}{\partial z} = -k_2 \frac{\partial T_2}{\partial z}$ $= h_1(T_1 - T_2)$
$z = z_2$	$-k_2 \frac{\partial T_2}{\partial z} = h_2(T_2 - T_{amb})$
$x = \pm\infty$	$T_1 = T_2 = T_{amb}$
$y = \pm\infty$	$T_1 = T_2 = T_{amb}$
$t = 0$	$T_1 = T_2 = T_{amb}$

Table 1: *Initial and boundary conditions.*

material between silicon and copper, and conductance h_2 represents an effective heat transfer coefficient [9, 29]. The power dissipated in transistors and wires is modeled by a prescribed heat flux $q(x,y,t)$ representing the 2D power density in the plane $z = 0$.

Temperature T is equal to $T_1(x,y,z,t)$ in layer 1, and $T_2(x,y,z,t)$ in layer 2. It verifies the following partial differential equation which is derived from Fourier's law and conservation of energy, assuming thermal conductivity is uniform in each layer [3, 21] :

$$\nabla^2 T_i = \frac{1}{\alpha_i} \frac{\partial T_i}{\partial t} \tag{1}$$

where ∇^2 is the Laplacian and α_i is the thermal diffusivity of layer i. Given initial and boundary conditions, the solution of equation (1) is unique [3]. Boundary and initial conditions are listed in Table 1.

The thermal conductivity varies with temperature, especially that of silicon. However, for simplifying the maths, it is common to assume a uniform thermal conductivity corresponding to a certain temperature range. In the remaining, unless stated otherwise, numerical

parameter	value	unit (SI)	meaning
k_1	100	W/mK	Si thermal conductivity
k_2	400	W/mK	Cu thermal conductivity
α_1	6×10^{-5}	m^2/s	Si thermal diffusivity
α_2	1.1×10^{-4}	m^2/s	Cu thermal diffusivity
h_1	40000	W/m^2K	interface material
h_2	500	W/m^2K	convection
z_1	0.0005	m	die thickness
$z_2 - z_1$	0.005	m	base-plate thickness
$L = \sqrt{A_{bp}}$	0.07	m	heat sink width

Table 2: *Parameter values used in numerical examples.*

examples use parameter values listed in Table 2. Conductivity k_1 and diffusivity α_1 correspond approximately to the characteristics of silicon around 100 °C. Values of k_2 and α_2 correspond to the characteristics of copper. Conductance h_1 corresponds to an interface resistance of $0.25K/W$ per cm^2. Conductance h_2 represents a heat sink cooled by forced convection of air. It corresponds to a thermal resistance

$$R_{hs} = \frac{1}{h_2 A_{bp}} = 0.4\,K/W$$

for a base-plate area $A_{bp} = 50\,cm^2$ (cf. Section 7). In this case, T_{amb} is the temperature of the air surrounding the heat sink [12].

The multi-layer model depicted in Figure 1 is a simplified view of reality. Microarchitects often must reason on systems with incomplete specification. When a parameter value is unknown, it is sometimes possible to set this parameter to a realistic value based on existing systems, and verify subsequently the impact of varying the parameter value on the microarchitectural decisions. This is easier on models featuring a small number of parameters. We believe that the model of Figure 1 provides a good trade-off between accuracy and number of parameters for microarchitecture studies.

Parameter values. Values in Table 2 are merely example values, yet realistic for an existing desktop system. Nevertheless, with analytical solutions, parameter values can be changed safely, so that the same model can be applied in different contexts. For example, we were able to reproduce the results of [29], which models a system with a heat spreader, two interfaces TIM1 and TIM2, and a heat sink base including a vapor chamber. This was possible by setting h_2 to simulate the effect of TIM2 and the wick structure, and by setting T_{amb} to the temperature of the top surface of the heat sink base.

3 Principle of superposition

An important characteristic of the model described in Section 2 is that it is a linear model. More precisely, Let $T_a(x,y,z,t)$ and $T_b(x,y,z,t)$ be the temperature corresponding to a heat flux $q_a(x,y,t)$ and $q_b(x,y,t)$ respectively. One can easily verify that $T(x,y,z,t) = T_a + T_b - T_{amb}$ is the solution of equation 1 corresponding to

$$q(x,y,t) = q_a(x,y,t) + q_b(x,y,t)$$

Defining the relative temperature $w_a = T_a - T_{amb}$, $w_b = T_b - T_{amb}$ and $w = T - T_{amb}$, we have

$$w(x,y,z,t) = w_a(x,y,z,t) + w_b(x,y,z,t) \tag{2}$$

Equation (2) defines the principle of superposition. It is a simple, yet very powerful statement. We use it extensively in the remaining of the paper. For example, it is sufficient to know the temperature generated by a point source : we can obtain the temperature for any power distribution by summing the contributions from each source separately. Moreover, the system is time-invariant, meaning that if $T(x,y,z,t)$ is the temperature corresponding to a heat flux $q(x,y,t)$, then $T_a(x,y,z,t-\tau)$ is the solution corresponding to $q_a(x,y,t-\tau)$. Hence it is possible to take advantage of the properties of linear time-invariant (LTI) systems [20].

The principle of superposition has been experimentally validated for a computer system in the case of natural and forced convection of air [14]. However, one must keep in mind that it is an approximation of reality : real boundary conditions are not exactly linear, material characteristics (especially silicon thermal conductivity) depend on temperature, and T_{amb} is neither uniform nor constant.

An important property of LTI systems is that the temperature generated by a time-varying power can be obtained from the temperature response to a constant power. Let us denote $w_q(x,y,t)$ the temperature on the plane $z = 0$ which is the response to a flux $q(x,y,t) = H(t) \times q(x,y)$, with $H(t)$ the unit step function defined as

$$H(t) = \begin{cases} 0 & t < 0 \\ 1 & t \geq 0 \end{cases}$$

For $t \leq 0$, w_q is null. Then for $t > 0$, w_q increases, until reaching a steady state value. Function $w_q(x,y,t)$ suffices to obtain the temperature response $w(x,y,0,t)$ to a time-varying power $p(t) \times q(x,y)$. In direct application of the superposition principle, $w(x,y,0,t)$ can be obtained by a convolution :

$$w(x,y,0,t) \quad = \quad \int_0^t p(\tau) \frac{\partial w_q}{\partial t}(x,y,t-\tau)\, d\tau \tag{3}$$

also known as Duhamel's theorem [3] (this can be proved by considering the identity $p(t) = \int_{-\infty}^{+\infty} p(\tau)\delta(t-\tau)\,d\tau$ and the fact that $\frac{\partial w_q}{\partial t}(x,y,t-\tau)$ is the temperature response to a power impulse $\delta(t-\tau)q(x,y)$).

A direct consequence of Duhamel's theorem is that the response to a sinusoid input $p(t)$, as $t \to \infty$, is a sinusoid output $w(t)$ with the same period (see Section 8). A periodic power $p(t)$ can be expressed as a Fourier series, so as $t \to \infty$, the temperature $w(t)$ is periodic with the same period as $p(t)$.

Duhamel's theorem can also be expressed in the Laplace domain. We recall the definition of the unilateral Laplace transform [3, 18, 20] :

$$\overline{p}(s) = \mathcal{L}\{p(t)\} = \int_0^\infty p(t)e^{-st}\,dt$$

Similarly we define $\overline{w_q}(s) = \mathcal{L}\{w_q(t)\}$ and $\overline{w}(x,y,z,s) = \mathcal{L}\{w(x,y,z,t)\}$. Then, recalling that w_q is null at $t = 0$, Duhamel's theorem can be written

$$\overline{w}(x,y,0,s) \quad = \quad s \times \overline{p}(s) \times \overline{w_q}(s) \tag{4}$$

It is sometimes easier to reason with Laplace-transformed quantities. For example, let us apply a power $P(t) \times q(x,y)$ with

$$P(t) = \int_0^t p(\tau)\,d\tau$$

Integration is simply a multiplication by $1/s$ in the Laplace domain. So $\overline{P}(s) = \mathcal{L}\{P(t)\} = \overline{p}(s)/s$. The temperature response is $\overline{w}(x,y,0,s)/s$, that is, in the time domain,

$$\int_0^t w(x,y,0,\tau)\,d\tau$$

If $p(t)$ is periodic of period t_0 with a null average on its period, then $P(t)$ is bounded. Hence the temperature corresponding to $P(t)$, that is, $\int_0^t w(x,y,0,\tau)\,d\tau$, is bounded too. So the average of $w(x,y,0,t)$ over t_0 becomes null as $t \to \infty$.

4 Laplace-transformed temperature for a point source and a step power

It is sufficient to obtain the temperature response to a point source dissipating a constant power $P \times H(t)$. Then, from spatial superposition and Duhamel's theorem, we can obtain the temperature for any power density $q(x,y,t)$.

The outline of the method we used to obtain the Laplace-transformed temperature for a point source is as follows :

- use a Laplace transform to remove the time-derivative in equation (1)
- assume a disk source to create a cylindrical symmetry and use cylindrical coordinates r, z
- use a Hankel transform to obtain an ordinary differential equation in z
- solve the ordinary differential equation in z
- apply a reverse Hankel transform
- make the disk radius infinitely small to obtain a point source

We assume a disk source of radius a on the plane $z = 0$, centered on the point $(0, 0, 0)$, dissipating a power $P \times H(t)$ uniformly. That is, $q(x, y, t) = H(t) \times P/(\pi a^2)$ inside the disk, $q(x, y, t) = 0$ outside. Using cylindrical coordinates and relative temperature, equation (1) can be written [3]

$$\frac{\partial^2 w_i}{\partial r^2} + \frac{1}{r}\frac{\partial w_i}{\partial r} + \frac{\partial^2 w_i}{\partial z^2} = \frac{1}{\alpha_i}\frac{\partial w_i}{\partial t} \tag{5}$$

with $r = \sqrt{x^2 + y^2}$ and $i \in \{1, 2\}$. We apply the Laplace transform :

$$\overline{w_i}(r, z, s) = \mathcal{L}\{w_i(r, z, t)\} = \int_0^\infty w_i(r, z, t)e^{-st}\, dt$$

and the Hankel transform [3, 21]

$$\overline{W_i}(\sigma, z, s) = \int_0^\infty r J_0(\sigma r)\overline{w_i}(r, z, s)\, dr$$

where J_0 is the Bessel function of the first kind of order 0. Equation (5) leads to

$$\frac{\partial^2 \overline{W_i}}{\partial z^2} = (\sigma^2 + \frac{s}{\alpha_i})\overline{W_i} \tag{6}$$

and boundary conditions in Table 1 become

$$\begin{aligned}
z = 0, \qquad & -k_1\frac{\partial \overline{W_1}}{\partial z} = \frac{P}{\pi a}\frac{J_1(\sigma a)}{\sigma s} \\
z = z_1, \qquad & -k_1\frac{\partial \overline{W_1}}{\partial z} = -k_2\frac{\partial \overline{W_2}}{\partial z} = h_1(\overline{W_1} - \overline{W_2}) \\
z = z_2, \qquad & -k_2\frac{\partial \overline{W_2}}{\partial z} = h_2\overline{W_2}
\end{aligned} \tag{7}$$

where J_1 is the Bessel function of the first kind of order 1. The general solution of (6) can be written in the form

$$\overline{W_i}(\sigma, z, s) = A_i(\sigma, s)e^{S_i(\sigma,s)z} + B_i(\sigma, s)e^{-S_i(\sigma,s)z}$$

with $S_i(\sigma, s)$ defined as

$$S_i(\sigma, s) = \sqrt{\sigma^2 + \frac{s}{\alpha_i}}$$

We have 4 unknowns A_1,B_1,A_2,B_2 that can be obtained by solving the system of 4 equations (7). Defining

$$\begin{aligned} e(\sigma, s) &= \frac{k_2 S_2 - h_2}{k2S_2 + h_2} e^{-2(z_2 - z_1)S_2} \\ f(\sigma, s) &= \frac{k_1 S_1}{h_1} + \frac{k_1 S_1}{k_2 S_2} \times \frac{1+e}{1-e} \\ g(\sigma, s) &= \frac{f-1}{f+1} e^{-2S_1 z_1} \end{aligned} \tag{8}$$

we obtain

$$\begin{aligned} A_1 &= \frac{P}{\pi a k_1 S_1} \frac{J_1(\sigma a)}{\sigma s} \times \frac{1}{1-g} \\ B_1 &= \frac{P}{\pi a k_1 S_1} \frac{J_1(\sigma a)}{\sigma s} \times \frac{g}{1-g} \end{aligned}$$

The temperature on the plane $z = 0$ is

$$\overline{W_1}(\sigma, 0, s) = A_1 + B_1 = \frac{P}{\pi a k_1 S_1} \frac{J_1(\sigma a)}{\sigma s} \times \frac{1+g}{1-g}$$

The space variable r can be recovered by a reverse Hankel transform [3, 21]

$$\begin{aligned} \overline{w_1}(r, 0, s) &= \int_0^\infty \sigma J_0(\sigma r) \overline{W_1}(\sigma, 0, s)\, d\sigma \\ &= \frac{P}{\pi a k_1 s} \int_0^\infty \frac{J_1(\sigma a) J_0(\sigma r)}{S_1(\sigma, s)} \times \frac{1 + g(\sigma, s)}{1 - g(\sigma, s)}\, d\sigma \end{aligned} \tag{9}$$

The solution for a point source dissipating a power $P \times H(t)$ can be obtained by taking the limit $a \to 0$. As $\lim_{a \to 0} \frac{J_1(\sigma a)}{a} = \frac{\sigma}{2}$, we get

$$\overline{w_1}(r, 0, s) = \frac{P}{2\pi k_1 r} \times \frac{\Phi(r, s)}{s} \tag{10}$$

with Φ defined as

$$\Phi(r,s) = r\int_0^\infty \frac{\sigma J_0(\sigma r)}{S_1(\sigma,s)} \times \frac{1+g(\sigma,s)}{1-g(\sigma,s)}\,d\sigma \tag{11}$$

Integration over an infinite interval is not practical, and we can take advantage of the exponential term in $g(\sigma,s)$

$$\Phi(r,s) \approx r\int_0^{5/z_1} \frac{\sigma J_0(\sigma r)}{S_1(\sigma,s)} \times \frac{1+g(\sigma,s)}{1-g(\sigma,s)}\,d\sigma + r\int_{5/z_1}^\infty \frac{\sigma J_0(\sigma r)}{S_1(\sigma,s)} \times\, d\sigma$$

that is, as $\int_0^\infty \frac{\sigma J_0(\sigma r)}{\sqrt{\sigma^2+s/\alpha_1}}\,d\sigma = \frac{1}{r}e^{-r\sqrt{s/\alpha_1}}$,

$$\Phi(r,s) \approx e^{-r\sqrt{s/\alpha_1}} + 2r\int_0^{5/z_1} \frac{\sigma J_0(\sigma r)}{S_1(\sigma,s)(\frac{1}{g(\sigma,s)}-1)}\,d\sigma \tag{12}$$

which can be evaluated with classical numerical integration methods. It should be noticed that the term $e^{-r\sqrt{s/\alpha_1}}$ in (12) is the value of Φ when $z_1 \to \infty$.

5 Sources of various shapes

The temperature for flat sources of various shapes in the plane $z = 0$ can be obtained by integrating formula (10). The temperature at the center of a disk of radius a dissipating a constant power $P \times H(t)$ uniformly is

$$\begin{aligned} \overline{w_{disk}}(P,a,s) &= \int_0^a \frac{\Phi(r,s)}{s} \times \frac{P/(\pi a^2)}{2\pi k_1 r} 2\pi r\,dr \\ &= \frac{P}{\pi a^2 k_1} \times \frac{\Psi(a,s)}{s} \end{aligned} \tag{13}$$

with Ψ defined as

$$\Psi(a,s) = \int_0^a \Phi(r,s)\,dr$$

Using the definition (11) of Φ, and because $\int_0^a rJ_0(\sigma r)\,dr = \frac{aJ_1(\sigma a)}{\sigma}$, we obtain

$$\Psi(a,s) = a\int_0^\infty \frac{J_1(\sigma a)}{S_1(\sigma,s)} \times \frac{1+g(\sigma,s)}{1-g(\sigma,s)}\,d\sigma$$

Note that we would have obtained the same formula by setting $r = 0$ in (9). As previously, we can take advantage of the exponential term in $g(\sigma,s)$. As $\int_0^\infty \frac{J_1(\sigma a)}{\sqrt{\sigma^2+s/\alpha_1}}\,d\sigma = \frac{1}{a}\sqrt{\frac{\alpha_1}{s}}(1 - e^{-a\sqrt{s/\alpha_1}})$, we obtain

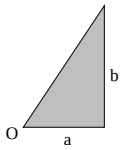

Figure 2: *Right triangle source dissipating a uniform power.*

$$\Psi(a,s) \approx \sqrt{\frac{\alpha_1}{s}}\left(1 - e^{-a\sqrt{s/\alpha_1}}\right) + 2a\int_0^{5/z_1} \frac{J_1(\sigma a)}{S_1(\sigma,s)(\frac{1}{g(\sigma,s)} - 1)}\, d\sigma \tag{14}$$

It should be noted that the left term in the sum (14) is the values of Ψ as $z_1 \to \infty$.

Quantity Ψ is useful also for obtaining the temperature at a vertex of a right triangle source. Figure 2 depicts a right triangle sources of sides a and b dissipating a uniform power P, that is, $q(x,y,t) = H(t) \times P/(\frac{1}{2}ab)$ inside the triangle, $q(x,y,t) = 0$ outside. We use polar coordinates (r,θ), taking vertex O as the origin. By integrating (10) over the triangle, we obtain the temperature at vertex 0 :

$$\begin{aligned}
\overline{w_{tri}}(P,a,b,s) &= \iint \frac{\Phi(r,s)}{s} \times \frac{q(r,\theta)}{2\pi k_1 r}\, r\, d\theta\, dr \\
&= \frac{P/(\frac{1}{2}ab)}{2\pi k 1 s}\int_0^{\tan^{-1}(b/a)} d\theta \int_0^{a/\cos\theta} \Phi(r,s)\, dr \\
&= \frac{P}{\pi ab k_1 s}\int_0^{\tan^{-1}(b/a)} \Psi(a/\cos\theta, s)\, d\theta
\end{aligned} \tag{15}$$

Quantity $\overline{w_{tri}}$ is useful for obtaining the temperature for polygonal sources. For example, the temperature inside a triangle source can be obtained by superposing six right triangles. However, for modeling power sources on a processor chip, the rectangle is the most practical shape. Let us consider a rectangle source of sides a and b dissipating 1 watt uniformly. The temperature at a vertex of the rectangle can be obtained by superposing two right triangles :

$$\overline{w_{1W}}(a,b,s) = \overline{w_{tri}}(0.5,a,b,s) + \overline{w_{tri}}(0.5,b,a,s)$$

Then, by superposing 4 rectangles, we can obtain the temperature at a point inside a rectangle source. We consider a rectangle source of sides a and b dissipating a power $P \times H(t)$ uniformly, centered on the point of coordinates $(0,0,0)$. The temperature at a point of coordinates $(x,y,0)$ is

$$\begin{aligned}\overline{w_{rec}}(P,a,b,x,y,s) = & \quad \mathcal{L}\{w_{rec}(P,a,b,x,y,t)\} \\ = & \quad P \times \Big[\quad (\frac{1}{2}+\frac{x}{a})(\frac{1}{2}+\frac{y}{b}) \times w_{1W}(|\frac{a}{2}+x|,|\frac{b}{2}+y|,s) + \\ & \quad (\frac{1}{2}-\frac{x}{a})(\frac{1}{2}+\frac{y}{b}) \times w_{1W}(|\frac{a}{2}-x|,|\frac{b}{2}+y|,s) + \\ & \quad (\frac{1}{2}+\frac{x}{a})(\frac{1}{2}-\frac{y}{b}) \times w_{1W}(|\frac{a}{2}+x|,|\frac{b}{2}-y|,s) + \\ & \quad (\frac{1}{2}-\frac{x}{a})(\frac{1}{2}-\frac{y}{b}) \times w_{1W}(|\frac{a}{2}-x|,|\frac{b}{2}-y|,s)\Big]\end{aligned} \tag{16}$$

It can be verified that (16) is valid also for points outside the rectangle. Hence, by superposition, it is possible to obtain the temperature at any point on the plane $z = 0$ when the power density map can be decomposed into a set of rectangle sources.

6 Transient and steady-state temperature response to a step power

6.1 Transient response

Obtaining the temperature as a function of time requires to invert the Laplace transform. In particular, we are searching the function $h(\sigma,t)$ whose Laplace transform is

$$\overline{h}(\sigma,s) \quad = \quad \mathcal{L}\{h(\sigma,t)\} = \frac{1}{s \times S_1(\sigma,s) \times (\frac{1}{g(\sigma,s)}-1)}$$

(this function is involved in formulas (12) and (14)).

There exists several numerical methods for inverting Laplace transforms [18]. We used the Gaver-Stehfest method [28], which permits recovering $h(t)$ approximately from $\overline{h}(s)$ sampled at a few points on the positive real axis. Indeed, the temperature response to a step power is a continuous, non-periodic, function of time, hence a Gaver-Stehfest method is appropriate. By comparison with a Fourier-series method for Laplace inversion [18], we found that a Gaver-Stehfest method with 10 samples is sufficient in practice to obtain $h(\sigma,t)$ with a reasonable accuracy.

The temperature as a function of time for a point source dissipating a constant power $P \times H(t)$ is (formula (10))

$$w_1(r,0,t) = \frac{P}{2\pi k_1 r} \times \mathcal{L}^{-1}\{\frac{\Phi(r,s)}{s}\} \tag{17}$$

where

$$\mathcal{L}^{-1}\{\frac{\Phi(r,s)}{s}\} \approx \operatorname{erfc}(\frac{r}{\sqrt{4\alpha_1 t}}) + 2r\int_0^{5/z_1} \sigma J_0(\sigma r)h(\sigma,t)\,d\sigma \tag{18}$$

where $\operatorname{erfc}(x) = \frac{2}{\sqrt{\pi}}\int_x^\infty e^{-u^2}\,du$ is the complementary error function. The temperature at the center of a disk source of radius a dissipating a constant and uniform power $P \times H(t)$ is (formula (13))

$$w_{disk}(P,a,t) = \frac{P}{\pi a^2 k_1} \times \mathcal{L}^{-1}\{\frac{\Psi(a,s)}{s}\} \tag{19}$$

where

$$\mathcal{L}^{-1}\{\frac{\Psi(a,s)}{s}\} \approx 2\sqrt{\frac{\alpha_1 t}{\pi}}\left(1 - e^{-\frac{a^2}{4\alpha_1 t}}\right) + a\operatorname{erfc}(\frac{a}{\sqrt{4\alpha_1 t}}) + 2a\int_0^{5/z_1} J_1(\sigma a)h(\sigma,t)\,d\sigma \tag{20}$$

Formula (20) permits obtaining the temperature $w_{tri}(P,a,b,t)$ at the vertex of a right triangle source, and by superposition, $w_{rec}(P,a,b,x,y,t)$. Although (18) and (20) are evaluated with numerical Laplace inversion and numerical integration in the general case, we can obtain simpler formulas for small times. In (17), the term

$$\frac{P}{2\pi k_1 r}\operatorname{erfc}(\frac{r}{\sqrt{4\alpha_1 t}}) \tag{21}$$

is the temperature we would obtain for $z_1 \to \infty$. In that case, since $\operatorname{erfc}(x)$ is very small for $x > 2$, all the energy released by the point source since $t = 0$ is located in a half sphere whose radius is approximately $\sqrt{16\alpha_1 t}$. For example, if the thickness of the silicon die is $z_1 = 0.5\,mm$, and taking α_1 as in Table 2, it takes $t = 260\,\mu s$ for the temperature on the opposite side of the silicon die to start increasing (slowly). Until this happens, formula (21) is valid in a half-sphere of radius z_1.

Now let us consider a point on the plane $z = 0$ and let us assume that the power density $q(x,y)$ is uniform and equal to q in the vicinity of the point. The temperature at the point can be obtained by integrating (21) :

$$\int_0^\infty \operatorname{erfc}(\frac{r}{\sqrt{4\alpha_1 t}}) \times \frac{q \times 2\pi r}{2\pi k_1 r}\,dr = \frac{2q}{k_1}\sqrt{\frac{\alpha_1 t}{\pi}} \tag{22}$$

which can also be obtained from (19) by taking $z_1 \to \infty$ and assuming $t < \frac{a^2}{16\alpha_1}$. It means that the transient temperature for small times is mainly a function of local power density and silicon characteristics. Other parameters, like the die thickness z_1, have an impact on the time during which (22) is valid.

Figure 3 shows the temperature at the center of a disk source of radius $1\,mm$ dissipating 1 watt uniformly for different values of z_1 (curves were obtained with formula (19)). The

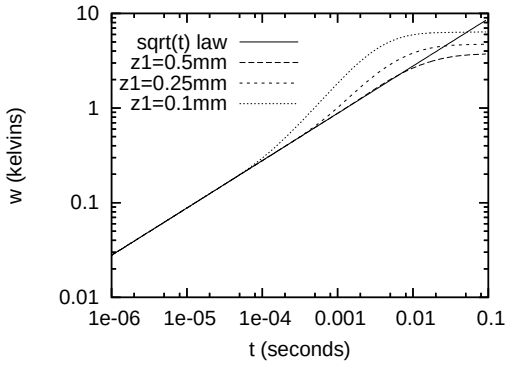

Figure 3: *Temperature at the center of a disk source of radius* $1\,mm$ *dissipating 1 watt uniformly, for* $z_1 = 0.5\,mm$,$z_1 = 0.25\,mm$ *and* $z_1 = 0.1\,mm$.

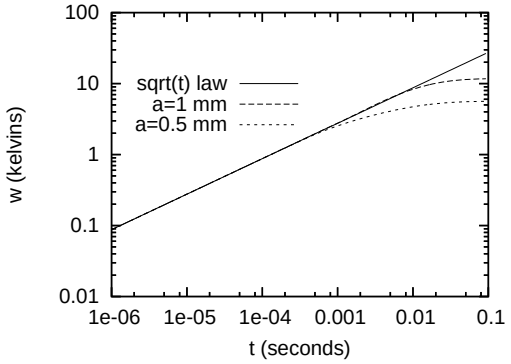

Figure 4: *Temperature at the center of a disk source of radius* $a = 1\,mm$ *and* $a = 0.5\,mm$ *dissipating* $1\,W/mm^2$.

$\sqrt{t}$ law (22) is also plotted on the graph. We see that the smaller z_1, the shorter the time during which (22) is valid. Moreover, it is interesting to notice that temperature increases as z_1 decreases.

Figure 4 shows the temperature at the center of a disk source of radius $a = 1\,mm$ and $a = 0.5\,mm$ with uniform power density $1\,W/mm^2$. The smaller the disk radius, the shorter the time during which (22) is valid.

It should be noted that the $\sqrt{t}$ law (22) implies that $\frac{\partial w_a}{\partial t}$ is infinite at $t = 0$. A similar observation was made in [19]. This effect comes from modeling heat generation with a planar source. Actually, heat generation in a chip occurs in a very thin layer. However, it

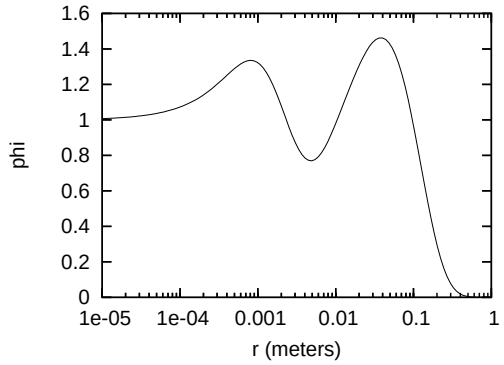

Figure 5: *Value of* $\Phi(r,0)$ *as a function of* r.

was shown in [24] that when the width and length of a volume source is more than 20 times greater than its thickness, the source behaves like a planar source.

6.2 Steady state

If we apply a constant power density $q(x,y)\times H(t)$, the corresponding temperature $w_q(x,y,t)$ on the plane $z=0$ increases until reaching a steady state $w_q(x,y,\infty)$.

Although temperature rises quickly at the beginning, it may take several minutes to reach a true steady state, depending on the mass of the heat sink.

We saw in Sections 4 and 5 how to obtain $\overline{w_q}(x,y,s) = \mathcal{L}\{w_q(x,y,t)\}$. We saw in Section 6.1 how to recover $w_q(x,y,t)$ from $\overline{w_q}(x,y,s)$. The steady state temperature can be obtained by taking a large value for t, e.g., several hundreds of seconds. However, the steady state temperature can also be obtained directly from the Laplace transform by applying the final-value theorem [18, 20] :

$$\lim_{t\to\infty} w_q(x,y,t) = \lim_{s\to 0} s \times \overline{w_q}(x,y,s)$$

For example, from (10), the steady-state temperature for a point source is

$$w_1(r,0,\infty) = \frac{P}{2\pi k_1 r}\Phi(r,0) \tag{23}$$

Figure 5 shows the value of $\Phi(r,0)$ as a function of r, obtained with formula (12) using the parameter values in Table 2. As can be observed, $\Phi(r,0)$ vanishes for $r > 40\,cm$. It means that sources at a distance greater than $40\,cm$ from a given point have almost no influence on the temperature at that point.

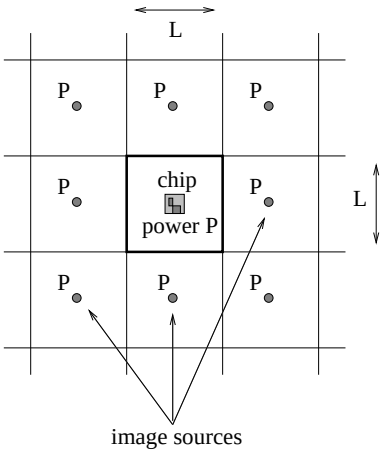

Figure 6: *An infinite number of image sources in the plane $z = 0$ simulate insulated walls at $x = \pm L/2$ and $y = \pm L/2$.*

7 Impact of the heat sink width

The model in previous sections assumes that the silicon and copper layers are infinite in the x and y directions. However, when h_2 is small, as is the case in Table 2, the limited base-plate area has a significant impact on the steady-state temperature. We assume that the base-plate is square, and that the chip is located at the center of the base-plate. The model of Figure 1 can be refined by considering that the two layers are delimited by insulated walls at $x = \pm L/2$ and $y = \pm L/2$, L being the base-plate width. Taking insulated walls is a common assumption justified by the fact that heat escaping by convection through the sides of the base-plate is negligible compared to that escaping through the top side.

The impact of lateral insulated walls can be taken into account by the method of images [3, 15]. Figure 6 illustrates the principle. The plane $z = 0$ is tiled with $L \times L$ squares. The chip, dissipating power P, is at the center of one of the squares representing the copper base plate. Images are point sources dissipating the same power P and placed at the center of each of the other squares. By using an infinite number of images, we create a symmetry that makes the heat flux vector at $x = \pm L/2$ and $y = \pm L/2$ parallel to the z-axis, which actually simulates insulated walls. [1] The contribution of a limited L to the temperature on the chip is

$$\Delta\overline{w}(P,s) = \mathcal{L}\{\Delta w(P,t)\} = \frac{P}{2\pi k_1 s} \sum_{(i,j)\neq(0,0)} \frac{\Phi(L\sqrt{i^2+j^2}, s)}{L\sqrt{i^2+j^2}} \tag{24}$$

[1] If we applied the method of image strictly, images should be exact copies of the chip. But in practice, the temperature contribution from a chip at distance L or greater is very close to that from a point source.

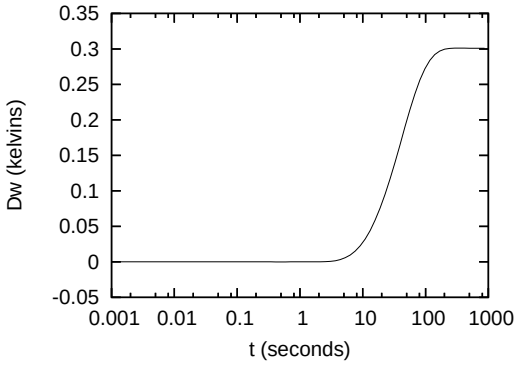

Figure 7: Value of $\Delta w(1,t)$ as a function of t.

In theory, the summation must be performed on an infinite number of images. In practice though, given the parameters of Table 2, it is sufficient to consider images at a distance less than $40\,cm$ from the chip (cf. Figure 5). The value $\Delta\overline{w}(P,s) = P \times \Delta\overline{w}(1,s)$ must be added to all the temperature numbers obtained with formulas in Sections 4 and 5.

Figure 7 shows the value of $\Delta w(P,t)$ as a function of t for $P = 1\,W$ and assuming $L = \sqrt{A_{bp}} = 7\,cm$. As can be observed, it takes several seconds for the effect of the limited heat sink width to start influencing temperature, and it takes more than 1 minute to reach a steady state. On this example, $\Delta w(1,\infty) \approx 0.3\,K/W$.

We are not aware of any conventional name for quantity $\Delta w(1,\infty)$. Layer 1 characteristics (z_1,k_1,h_1) have little impact on $\Delta w(1,\infty)$, which mostly characterizes the heat sink, like R_{hs} (cf. Section 2. But unlike R_{hs}, $\Delta w(1,\infty)$ takes into account not only the conductance h_2 and the base-plate width, but also the base-plate thickness and thermal conductivity.

8 Frequency response

8.1 Sinusoid power

From Section (3), if $w_q(x,y,t)$ is the temperature response to a power $H(t)q(x,y)$, then the temperature response $w(x,y,t)$ to a power $p(t)q(x,y)$ is

$$\begin{aligned} w(x,y,t) &= \int_0^t p(\tau)\frac{\partial w_q}{\partial t}(x,y,t-\tau)\,d\tau \\ &= \int_0^t p(t-\tau)\frac{\partial w_q}{\partial t}(x,y,\tau)\,d\tau \end{aligned}$$

In particular, the response to a complex signal $p(t) = H(t) \times e^{i2\pi ft}$ (where $i = \sqrt{-1}$) is

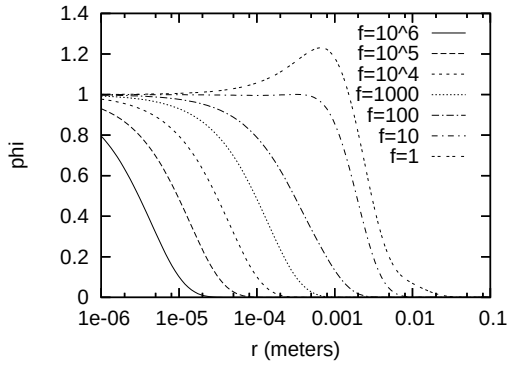

Figure 8: Value of $|\Phi(r, i2\pi f)|$ as a function of r for different values of f (in hertz).

$$w(x,y,t) \quad = \quad e^{i2\pi ft} \int_0^t e^{-i2\pi f\tau} \frac{\partial w_q}{\partial t}(x,y,\tau)\, d\tau$$

As $t \to \infty$, the steady-state behavior is

$$w(x,y,t) \sim e^{i2\pi ft} \times \mathcal{F}(f) \tag{25}$$

where $\mathcal{F}(f)$ is a complex number independent of time

$$\begin{aligned} \mathcal{F}(f) &= \mathcal{L}\{\frac{\partial w_q}{\partial t}\}(x,y,i2\pi f) \\ &= i2\pi f \times \overline{w_q}(x,y,i2\pi f) \end{aligned} \tag{26}$$

Relation (25) shows that the temperature response to a sinusoid power converges to a sinusoid (the real and imaginary parts of $w(x,y,t)$ converge respectively to the real and imaginary parts of $e^{i2\pi ft} \times \mathcal{F}(f)$). The modulus of $\mathcal{F}(f)$ is the amplitude of the temperature oscillation.

In other words, if $\overline{w_q}(x,y,s)$ is the Laplace transform of the temperature response to a step power $H(t) \times q(x,y)$, the steady-state frequency response can be obtained by setting $s = i2\pi f$ in $s \times w_q(x,y,s)$. For example, from (10), the amplitude of the temperature oscillation generated by a point source dissipating a power $P \times H(t)e^{i2\pi ft}$ is

$$|i2\pi f \times \overline{w_1}(r,0,i2\pi f)| = \frac{P}{2\pi k_1 r} \times |\Phi(r, i2\pi f)| \tag{27}$$

Figure 8 shows the value of $|\Phi(r, i2\pi f)|$ as a function of r for different values of f (in hertz). As can be observed, for a given frequency f, there exists a value of r beyond which the temperature oscillation is practically null. For example, in Figure 8, frequencies greater than $1000\,Hz$ are filtered out at a distance greater than $1\,mm$ from the point source. Actually, for $f > 100\,Hz$, the first term in (12) dominates, and we have

$$|\Phi(r, i2\pi f)| \approx e^{-r\sqrt{\pi f/\alpha_1}} \tag{28}$$

which is the value corresponding to $z_1 = \infty$. The temperature oscillation decreases exponentially with the distance from the source. In practice, for $r > 10\sqrt{\alpha_1/(\pi f)}$, it is almost nonexistent.

8.2 Power that is periodically on and off

In a microprocessor, a periodic power is more likely to resemble a square wave than a sinusoid. Hence it is interesting to study the case of a power that is periodically on and off.

Let us consider a power density map $q(x, y)$, and $w_q(x, y, t)$ the temperature response to a step power $q(x, y)H(t)$. We consider the following time-varying power of period τ and duty factor $\gamma \in [0, 1]$:

$$q(x, y, t) = q(x, y) \sum_{n \geq 0} \Big(H(t - n\tau) - H(t - n\tau - \gamma\tau) \Big)$$

That is, power is successively on and off for $\gamma\tau$ and $(1 - \gamma)\tau$ respectively. We denote $w_o(t)$ the temperature at point $O(x_o, y_o, 0)$ as a response to $q(x, y, t)$. Response $w_o(t)$ can be computed as the sum of the response to a step power $\gamma q(x, y)H(t)$ and the response to the oscillating part of $q(x, y, t)$ defined as

$$\begin{aligned} \widetilde{q}(x, y, t) &= q(x, y, t) - \gamma q(x, y)H(t) \\ &= q(x, y) \sum_{n \geq 0} \Big((1 - \gamma)H(t - n\tau) + \gamma H(t - (n + 1)\tau) - H(t - (n + \gamma)\tau) \Big) \end{aligned}$$

We denote $\widetilde{w_o}(t)$ the contribution of $\widetilde{q}(x, y, t)$ to $w_o(t)$. It should be noted that the time-average of $\widetilde{q}(x, y, t)$ over period τ is null, so the time-average of $\widetilde{w_o}(t)$ becomes null as $t \to \infty$ (Section 3). From the superposition principle, we have

$$\widetilde{w_o}(t) = \sum_{n \geq 0} \Big((1-\gamma)w_q(x_o, y_o, t-n\tau) + \gamma w_q(x_o, y_o, t-(n+1)\tau) - w_q(x_o, y_o, t-(n+\gamma)\tau) \Big) \tag{29}$$

From Figure 8, if τ is less than $1\,ms$ (i.e., the oscillation frequency is greater than 1000 Hz), we can practically consider that only the power sources at a distance less than $1\,mm$ from point O contribute to $\widetilde{w_o}(t)$.

Let us assume that power density $q(x,y)$ is uniform and equal to q_o in a disk of radius $1\,mm$ centered on O. The frequency response is practically that obtained with $z_1 = \infty$ (Section 8.1). So in formula (29), we can approximate $w_q(x_o, y_o, t)$ with expression (22). We obtain

$$\widetilde{w_o}(t) \approx \frac{2q_o}{k_1}\sqrt{\frac{\alpha_1}{\pi}}\Big((1-\gamma)\sum_{n=0}^{\lfloor t/\tau \rfloor}\sqrt{t-n\tau} + \gamma\sum_{n=0}^{\lfloor t/\tau \rfloor - 1}\sqrt{t-(n+1)\tau} - \sum_{n=0}^{\lfloor t/\tau - \gamma \rfloor}\sqrt{t-(n+\gamma)\tau}\Big)$$

The maximum of the oscillation occurs at times $t = (m+\gamma)\tau$, m being integer :

$$\begin{aligned}\widetilde{w_o}((m+\gamma)\tau) &\approx \frac{2q_o}{k_1}\sqrt{\frac{\alpha_1}{\pi}}\Big((1-\gamma)\sum_{n=0}^{m}\sqrt{(m+\gamma-n)\tau} + \gamma\sum_{n=0}^{m-1}\sqrt{(m+\gamma-n-1)\tau} \\ &\qquad - \sum_{n=0}^{m}\sqrt{(m-n)\tau}\Big) \\ &= \frac{2q_o}{k_1}\sqrt{\frac{\alpha_1\tau}{\pi}}\Big((1-\gamma)\sqrt{\gamma} + \sum_{n=1}^{m}[(1-\gamma)\sqrt{n+\gamma} + \gamma\sqrt{n+\gamma-1} - \sqrt{n}]\Big)\end{aligned}$$

Taking $m \to \infty$, we obtain

$$\begin{aligned}&\sum_{n=1}^{\infty}[(1-\gamma)\sqrt{n+\gamma} + \gamma\sqrt{n+\gamma-1} - \sqrt{n}] = \\ &\qquad (1-\gamma)\sqrt{1+\gamma} + \gamma\sqrt{\gamma} - 1 + \sum_{n=2}^{\infty}\sqrt{n}\Big[(1-\gamma)\sqrt{1+\frac{\gamma}{n}} + \gamma\sqrt{1-\frac{1-\gamma}{n}} - 1\Big]\end{aligned}$$

Using the Taylor series approximation $\sqrt{1+x} \approx 1 + \frac{x}{2} - \frac{x^2}{8}$, the infinite sum is approximately

$$-\frac{\gamma(1-\gamma)}{8}\sum_{n=2}^{\infty}\frac{1}{n\sqrt{n}} \approx -\frac{\gamma(1-\gamma)}{8} \times 1.6124$$

So

$$\widetilde{w_o}((m+\gamma)\tau) \approx \frac{2q_o}{k_1}\sqrt{\frac{\alpha_1\tau}{\pi}}\Big(\sqrt{\gamma} + (1-\gamma)\sqrt{1+\gamma} - 1 - \frac{\gamma(1-\gamma)}{8} \times 1.6124\Big)$$

A simpler approximation is

$$\widetilde{w_o}((m+\gamma)\tau) \approx \frac{2q_o}{k_1}\sqrt{\frac{\alpha_1\tau}{\pi}}\sqrt{\gamma(1-\gamma)(1-\sqrt{\gamma})} \quad (30)$$

The minimum of the oscillation can be found by a similar computation. As $m \to \infty$,

$$\widetilde{w_o}(m\tau) \approx \frac{2q_o}{k_1}\sqrt{\frac{\alpha_1\tau}{\pi}}\Big(1-\gamma-\sqrt{1-\gamma}-\frac{\gamma(1-\gamma)}{8}\sum_{n=2}^{\infty}\frac{1}{n\sqrt{n}}\Big)$$

which is a negative number. The amplitude of the oscillation as $m \to \infty$ is

$$\widetilde{w_o}((m+\gamma)\tau) - \widetilde{w_o}(m\tau) \approx \frac{2q_o}{k_1}\sqrt{\frac{\alpha_1\tau}{\pi}}\Big(\sqrt{\gamma}+(1-\gamma)\sqrt{1+\gamma}-2+\gamma+\sqrt{1-\gamma}\Big)$$

A rougher approximation is

$$\widetilde{w_o}((m+\gamma)\tau) - \widetilde{w_o}(m\tau) \approx \frac{2q_o}{k_1}\sqrt{\frac{\alpha_1\tau}{\pi}}\sqrt{\gamma(1-\gamma)} \quad (31)$$

9 Examples

Formulas in previous sections can be used to reason about temperature in microprocessors. They can also be implemented in a performance/power microarchitecture simulator. This section provides two examples illustrating these possible uses.

9.1 Thread migration on a multi-core

Let us consider a processor with N cores numbered from 1 to N. We assume that each core i dissipates a uniform time-average power P_i. For simplicity, we neglect the power dissipated outside cores, e.g., shared caches and buses. From the principle of superposition, the steady-state time-average relative temperature w_i in core i is

$$w_i = \sum_{j=1}^{N} P_j \times w_{ij} \quad (32)$$

where $w_{ij} > 0$ is the steady-state relative temperature in core i per watt generated in core j.

If cores i and j, $i \neq j$, are not too close to each other, w_{ij} can be approximated as the temperature generated by a point source generating 1 watt and located in core j. Hence from the principle of reciprocity for point sources (see Appendix A), we have approximately $w_{ij} = w_{ji}$, i.e., matrix (w_{ij}) is symmetric.

Let us apply a uniform power $P_i = P/N$, with P the total power. Relation (32) yield

$$w_i = \frac{P}{N} \times \sum_{j=1}^{N} w_{ij}$$

We say that cores are *thermally equivalent* if w_{ii} and the sum

$$R_{ja} = \frac{1}{N} \sum_{j=1}^{N} w_{ij} = \frac{1}{N} \sum_{j=1}^{N} w_{ji}$$

do not depend on i. In this case [2]

$$w_i = P \times R_{ja} \tag{33}$$

Quantity R_{ja}, measured in kelvins/watt, is commonly called *junction-to-ambient thermal resistance*. Thermal equivalence of cores implies that when the same power is applied on each core, they have the same temperature. It also implies that all the rows of the symmetric matrix (w_{ij}) are obtained by a permutation on the first row. Hence the N values w_{1j} are sufficient to obtain the steady-state temperature on each core.

It should be noted that relation (33) can be generalized to a non-uniform power provided we consider the spatial-average temperature defined as

$$w_{avg} = \frac{1}{N} \sum_{i=1}^{N} w_i$$

From (32), we have

$$w_{avg} = \sum_{j=1}^{N} P_j \frac{1}{N} \sum_{i=1}^{N} w_{ij} = P \times R_{ja} \tag{34}$$

where $P = \sum_{j=1}^{N} P_j$ is the total power.

If power is non-uniform though, temperature is non-uniform as well. The peak temperature is higher than the spatial-average temperature. A possible solution for minimizing the peak temperature is to migrate threads so that each core "sees" all threads periodically. For example, periodically, we can migrate all threads at once in a circular fashion : the thread that was running on core 1 goes to core 2, the thread previously on core 2 goes to core 3, and so on.

If we migrate frequently enough, the amplitude of the temperature oscillation on each core is negligible (cf. Section 8) and temperature is always close to its time-average value. Thread migrations make power, hence temperature, uniform.

[2] In practice, thermal equivalence of cores is approximately verified on 2-core and 4-core processors, provided cores are identical and the chip layout is reasonably symmetric. With more than 4 cores, ensuring thermal equivalence, even approximately, is more constraining (e.g., cores located at the vertices of a regular polygon)

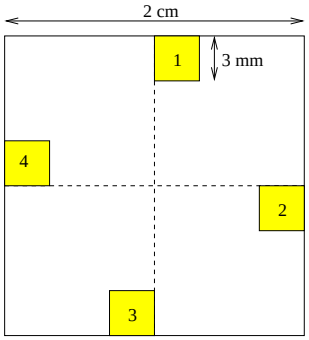

Figure 9: *Example of 4-core chip. Cores dissipate a uniform power.*

Numerical example. Let us consider the 4-core chip depicted in Figure 9, where each core is modeled as a $3mm$-side square dissipating a uniform power. Given the parameter values in Table 2, and using Formula (16), we obtain (cf. Section 6.2)

$$\begin{aligned} w_{11} &\approx 2.63\,K/W \\ w_{12} &\approx 0.44\,K/W \\ w_{13} &\approx 0.42\,K/W \\ w_{14} &= w_{12} \\ R_{ja} &= \frac{1}{4}\sum_j w_{1j} \approx 0.98\,K/W \end{aligned}$$

It should be noted that values w_{ij} take into account the contribution $\Delta w(1,\infty)$ from the finite heat sink width, which is $0.3\,K/W$ here (cf. Section 7).

Matrix (w_{ij}) is

$$\begin{pmatrix} w_{11} & w_{12} & w_{13} & w_{14} \\ w_{12} & w_{11} & w_{14} & w_{13} \\ w_{13} & w_{14} & w_{11} & w_{12} \\ w_{14} & w_{13} & w_{12} & w_{11} \end{pmatrix}$$

For example, let consider 4 threads, two of which dissipate $20\,W$ and the two others dissipate $10\,W$. For instance, we can put the most dissipating threads on cores 1 and 3. If threads keep executing on fixed cores, we obtain the following temperatures :

$$\begin{pmatrix} w_1 \\ w_2 \\ w_3 \\ w_4 \end{pmatrix} = \begin{pmatrix} w_{11} & w_{12} & w_{13} & w_{14} \\ w_{12} & w_{11} & w_{14} & w_{13} \\ w_{13} & w_{14} & w_{11} & w_{12} \\ w_{14} & w_{13} & w_{12} & w_{11} \end{pmatrix} \times \begin{pmatrix} 20 \\ 10 \\ 20 \\ 10 \end{pmatrix} = \begin{pmatrix} 69.8 \\ 48.1 \\ 69.8 \\ 48.1 \end{pmatrix}$$

The temperature difference between hot and cold cores exceeds $20\,K$ on this example. The spatial-average relative temperature is $(69.8 \times 2 + 48.1 \times 2)/4 \approx 59\,K$. From (34), and assuming the power consumed by migrations brings a negligible temperature contribution, $59\,K$ is the lowest peak temperature we can achieve by migrating threads. That is, thread migration decreases temperature by as much as $69.8 - 59 = 10.8\,K$.

The reasoning above is for the time-average power and time-average temperature. When migrating threads, we have a temperature oscillation. We want the amplitude of this oscillation to be much smaller than the potential temperature decrease of $10.8\,K$.

Each core "sees" consecutively and periodically $20\,W$ and $10\,W$. The time-varying power is a square-wave whose period τ is twice the time between consecutive migrations. The temperature oscillation on a core i is almost completely determined by the power density oscillation on core i, as distant power oscillations are filtered out (cf. Section 8.1).

The power density generated by the $20\,W$ threads is $q_{high} = 20/9 = 2.2\,W/mm^2$. The power density generated by the $10\,W$ threads is $q_{low} = 10/9 = 1.1\,W/mm^2$. We can use formula (30) with $q_o = q_{high} - q_{low} = 1.1\,W/mm^2$ and $\gamma = 0.5$. We want $\widetilde{w_o}((m+\gamma)\tau)$ to be much smaller than $10.8\,K$, let us say smaller than $0.5\,K$. We find

$$\begin{aligned} \tau &< \frac{\pi}{\alpha_1}\Big(\frac{k_1 \times 0.5}{2q_o\sqrt{\gamma(1-\gamma)(1-\sqrt{\gamma})}}\Big)^2 \\ &\approx 370\,\mu s \end{aligned}$$

Hence the migration interval should be $185\,\mu s$ or less.

9.2 Thermal management with a temperature sensor

The performance of a temperature-constrained processor depends on the temperature measures given by the integrated thermal sensors, as thermal sensors trigger actions that impact power consumption.

Performance/power microarchitecture simulators generally model power at the level of microarchitectural units. Figure 10 shows a chip layout inspired from the IBM PowerPC 970FX, where we show the main units. Lacking further information, we model units as rectangle-shaped regions with a uniform power density.

Let us assume that we have N rectangles numbered from 1 to N. Rectangle i dissipates a uniform power density $q_i(t)$. Its area is A_i. The total power is

$$P(t) = \sum_{i=1}^{N} A_i \times q_i(t)$$

Let us assume that we have a single thermal sensor located in rectangle 1 (this discussion could be generalized to multiple sensors). We denote $w_i(t)$ the relative temperature generated at the sensor when we apply $1\,W/mm^2$ in rectangle i. From superposition and Duhamel's theorem (3), the relative temperature $w(t)$ at the sensor is

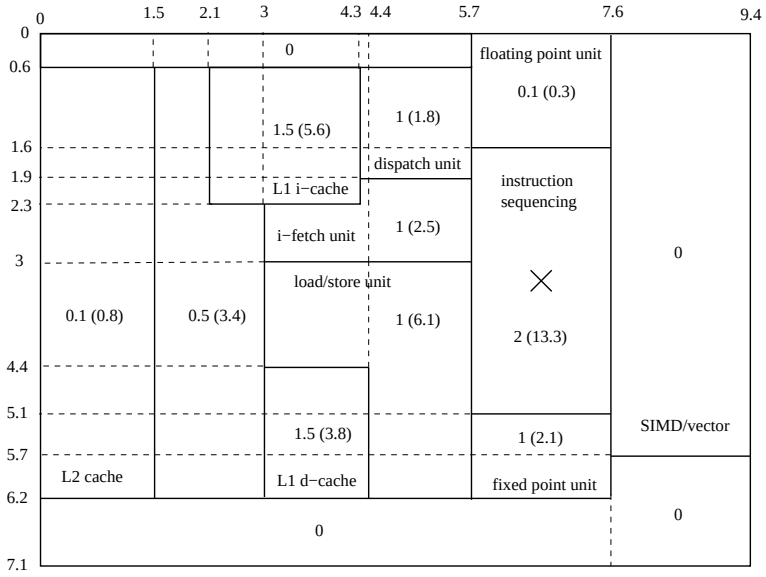

Figure 10: *Example of chip layout, taken from the IBM PowerPC 970FX. Numbers on the top and left of the figure represent coordinates in* mm*. Numbers in each region represent (random) power densities in* W/mm^2*, with the corresponding number of watts in parentheses. We assume that there is a thermal sensor at the point marked by a cross.*

$$w(t) = \sum_{i=1}^{N} \int_0^t q_i(\tau) \frac{dw_i}{dt}(t-\tau)\, d\tau \tag{35}$$

In practice, power models work with a fixed time-step Δt. That is to say, for any integer n, power density $q_i(t)$ is assumed constant and equal to $q_i(n\Delta t)$ between $n\Delta t$ and $(n+1)\Delta t$. From (35), we get

$$w(mt) = \sum_{i=1}^{N} \sum_{n=0}^{m-1} q_i(n\Delta t) \times [w_i((m-n)\Delta t) - w_i((m-n-1)\Delta t)] \tag{36}$$

for any integer m. Formula (36) can be integrated in a performance/power microarchitecture simulator. Values $w_i(n\Delta t)$ are computed with (16) and (24) and can be stored in an array to avoid recomputing them several times. Moreover, it is not necessary to use (16) and (24) for all values of n. We can compute $w_i(t)$ for a few tens of points, and perform a polynomial interpolation, which is faster.

At every time-step, we compute the temperature based on past power events. In the general case, we cannot use FFT-based convolution to speed-up (36), because power events in a thermally-constrained processor may depend on temperature, as in the example below.

However, in practice, it is possible to decrease the number of events with little loss of accuracy. For example, if $q_i(t)$ is approximately constant for several consecutive time-steps, it is possible to define a single power event spanning these time-steps.

Also, it is possible to merge power events that are remote in time or in space. Let us assume that for $n \in [n_1, n_2]$, $\frac{dw_i}{dt}((m-n)\Delta t)$ is approximately constant. Then

$$\sum_{n=n_1}^{n_2-1} q_i(n\Delta t) \times [w_i((m-n)\Delta t) - w_i((m-n-1)\Delta t)] \approx \frac{w_i((m-n_1)\Delta t) - w_i((m-n_2)\Delta t)}{n_2 - n_1} \sum_{n=n_1}^{n_2-1} q_i(n\Delta t) \tag{37}$$

Consequently, we can define a single power event from $n_1\Delta t$ to $n_2\Delta t$ whose value is the time-average power density

$$\frac{1}{n_2 - n_1} \sum_{n=n_1}^{n_2-1} q_i(n\Delta t)$$

In practice, after a certain time, the second derivative of the response $w_i(t)$ decreases in absolute value. Hence for a fixed n_2, and as m increases, n_1 can be taken smaller. That is, as time increases, it is possible to merge a larger number of past events. This can be done progressively, by comparing the value of $[w_i((m-n_1-1)\Delta t) - w_i((m-n_1)\Delta t)]$ with that of $[w_i((m-n_1)\Delta t) - w_i((m-n_2)\Delta t)]/(n_2-n_1)$.

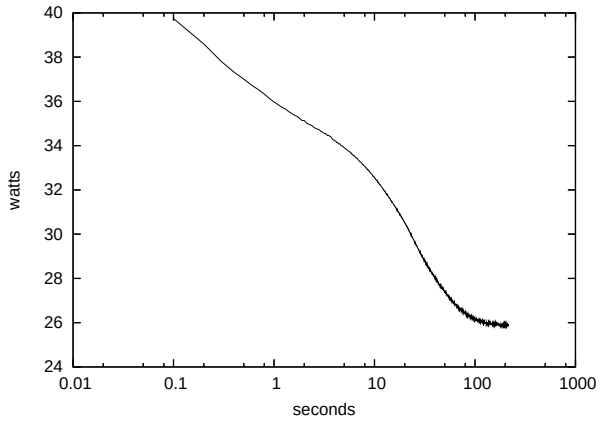

Figure 11: *Power dissipated as a function time.*

Also, when a power source is remote in space, it takes some time for $w_i(t)$, $i \neq 1$, to start increasing. And when $w_i(t)$ increases, it does so much more slowly than $w_1(t)$. Hence it is possible to use a different time-step for remote sources, or equivalently, to merge power events as described above.

Experiment. We applied in each unit of the PowerPC 970FX the power densities that are indicated in Figure 10 (these are random numbers, for the sake of example). The total power consumption is $39.75, W$. The sensor is located at the center of the instruction sequencing unit.

Without any constraint on the maximum relative temperature, the steady-state relative temperature at the center of the instruction sequencing unit is approximately $60.5\,K$, of which $\Delta w(39.75, \infty) \approx 12\,K$ come from the finite heat sink width and $35 + \Delta w(39.75, \infty) = 47\,K$ come from the instruction sequencing unit alone.

Now we assume that the relative temperature is limited to a maximum value of $w_{max} = 40\,K$. When the relative temperature exceeds w_{max}, we stop the processor for $100\,\mu s$, which is 10 time-steps assuming $\Delta t = 10\,\mu s$. With this on-off mechanism, the time-average power is automatically regulated so that the relative temperature stays close to w_{max}. Figure 11 shows the total power as a function of time. Initially, the chip is at the ambient temperature, i.e., the relative temperature is null. As long as relative temperature is less than w_{max}, power is maximum and equal to $39.75\,W$. Once w_{max} is reached, which happens at $t \approx 0.1\,s$, the on-off mechanism triggers repeatedly, and more frequently as time increases : power consumption decreases, until we reach a steady state. The steady-state power on this example is $39.75 \times 40/60.5 \approx 26\,W$.

10 Related works and conclusion

We believe that our approach, based on point sources, principle of superposition, and method of images, provides an intuitive basis for reasoning about temperature.

Although the model was primarily developed for reasoning and gaining understanding, analytical formulas can also be implemented in performance/power microarchitecture simulators, as illustrated in Section 9.2.

The analytical formulas permit obtaining quickly the steady-state temperature or the transient temperature response, at any point on the dissipating plane. Closed-form approximations like (22) or (30) can be used for quickly reasoning about the transient temperature behavior for short times. Other more complex formulas, like (10) or (16), can be programmed easily, e.g., in C (as we did), or with a mathematics software.

Multi-layer models like ours have long been used to model the transient or steady-state temperature in integrated circuits [13, 1, 15, 19, 5, 7, 2, 25] (the list is not exhaustive). These models differ in the number of layers, contact between layers, boundary conditions, power generation, temperature dependence of thermal properties, etc.

Our model is based on several simplifying assumptions (Sections 2 and 7) and is less detailed than some previously published models, like [2], that assumes a complex geometry, thermal non linearity, volume sources and general boundary conditions.

One of the specificities of temperature modeling for microarchitecture research is that the exact temperature on a chip depends on a large number of parameters, e.g. the shape, position, and power consumption of the millions of transistors and wires. These parameters are generally not known when defining a new microarchitecture. Hence the accuracy of temperature models used by microarchitects is inherently limited. Our goal is to obtain a temperature model that is "qualitatively" accurate, i.e., such that an engineer can take correct decisions. The model proposed in this report is a step in that direction.

Although we defined our model as a 2-layer model, thermal conductances h_1 and h_2 permit emulating 4 layers with perfect contact. In theory, there is no limitation on the number of layers that can be modeled analytically [7, 18]. Yet, it is not sure whether modeling more layers is really necessary for microarchitecture studies. We believe that the most important improvement would be to take into account thermal non linearity via Kirchhoff transformation [3, 21, 15, 2], as the effects of non linearity can be significant in silicon devices [2].

A Principle of reciprocity

The principle of reciprocity for point sources means that the steady-state temperature at point M_2 generated by a point source located at point M_1 equals the steady-state temperature at M_1 when the same source is located at M_2.

If one considers infinite layers as in Figure 1, this is obviously true, for reasons of symmetry. However, this remains true in more general cases.

Let us consider a solid of volume V delimited by a surface S and consisting of a material which may be heterogeneous. The solid is surrounded by an ambient medium at temperature T_{amb}. We assume that there is no heat generated inside the solid. Hence at steady state and at each point in the solid, the divergence of the heat flux vector $\vec{q}$ is null, that is,

$$\vec{\nabla} \cdot \vec{q} = 0$$

where $\vec{\nabla}$ is the *nabla* notation for the gradient.

On a fixed part of S, we apply a surface power density $\vec{q} \cdot \vec{n}$ where $\vec{n}$ is the outward normal unit vector (by convention, we have $\vec{q} \cdot \vec{n} \geq 0$ when heat leaves the solid). We denote S_q this part of S where we apply a power density. On the remaining part of S, which we denote S_h, we assume that

$$\vec{q} \cdot \vec{n} = h \times w$$

where h is a heat transfer coefficient (not necessarily uniform over S_h) and $w = T - T_{amb}$ is the relative temperature on the surface of the solid.

Fourier's law can be written

$$\vec{q} = -k\vec{\nabla}w$$

where k is the thermal conductivity, which is not necessarily uniform and may depend on temperature.

Now let us consider two power densities $\vec{q_1} \cdot \vec{n}$ and $\vec{q_2} \cdot \vec{n}$ over S_q, and w_1 and w_2 the steady-state relative temperature corresponding to each power density respectively. We have

$$\begin{aligned}
\iint_{S_q} w_2\vec{q_1} \cdot \vec{n}\, dS &= \iint_{S} w_2\vec{q_1} \cdot \vec{n}\, dS - \iint_{S_h} w_2\vec{q_1} \cdot \vec{n}\, dS \\
&= \iiint_{V} \vec{\nabla} \cdot w_2\vec{q_1}\, dV - \iint_{S_h} hw_1w_2\, dS \\
&= \iiint_{V} w_2\vec{\nabla} \cdot \vec{q_1}\, dV + \iiint_{V} \vec{\nabla}w_2 \cdot \vec{q_1}\, dV - \iint_{S_h} hw_1w_2\, dS \\
&= -\iiint_{V} k\vec{\nabla}w_1 \cdot \vec{\nabla}w_2\, dV - \iint_{S_h} hw_1w_2\, dS
\end{aligned}$$

where we have applied the divergence theorem. The expression on the right-hand side is symmetric with respect to w_1 and w_2, hence we have

$$\iint_{S_q} w_2\vec{q_1} \cdot \vec{n}\, dS = \iint_{S_q} w_1\vec{q_2} \cdot \vec{n}\, dS \tag{38}$$

It should be noted that (38) was derived without making any assumptions on power densities $\vec{q_1} \cdot \vec{n}$ and $\vec{q_2} \cdot \vec{n}$. Now let us assume that power density $\vec{q_1} \cdot \vec{n}$ corresponds to a point source

dissipating a power P and located at point $M_1 \in S_q$ (i.e., $\vec{q}_1 \cdot \vec{n}$ is null everywhere on S_q except in an infinitely small area surrounding M_1), and $\vec{q}_2 \cdot \vec{n}$ corresponds to a point source dissipating the same power P and located at point $M_2 \in S_q$. From (38), we obtain

$$w_2(M_1) = w_1(M_2) \tag{39}$$

which is the principle of reciprocity for point sources.

The principle of reciprocity can be extended to sources of random shapes dissipating the same uniform power, provided one considers spatial-average temperatures. Let us consider $\vec{q}_1 \cdot \vec{n}$ uniform and equal to P/S_1 inside $S_1 \subset S_q$ and null outside. Similarly, we consider $\vec{q}_2 \cdot \vec{n}$ uniform and equal to P/S_2 inside $S_2 \subset S_q$ and null outside. From (38), we have

$$\iint_{S_1} w_2 \frac{P}{S_1}\, dS = \iint_{S_2} w_1 \frac{P}{S_2}\, dS$$

that is,

$$\frac{1}{S_1} \iint_{S_1} w_2\, dS = \frac{1}{S_2} \iint_{S_2} w_1\, dS$$

References

[1] P. Antognetti, G.R. Bisio, F. Curatelli, and S. Palara. Three-dimensional transient thermal simulation : application to delayed short circuit protection in power IC's. *IEEE Journal of Solid-State Circuits*, SC-15(3):277–281, June 1980.

[2] W. Batty, C.E. Christoffersen, A.J. Panks, S. David, C.M. Snowden, and M.B. Steer. Electro-thermal CAD of power devices and circuits with fully physical time-dependent compact thermal modelling of complex non linear 3-dimensional systems. *IEEE Transactions on Components and Packaging Technologies*, 24(4):566–590, December 2001.

[3] H.S. Carslaw and J.C. Jaeger. *Conduction of heat in solids*. Oxford University Press, 1959.

[4] P. Chaparro, J. González, and A. González. Thermal-effective clustered microarchitectures. In *First Workshop on Temperature-Aware Computer Systems (TACS-1)*, 2004.

[5] D.H. Chien, C.Y. Wang, and C.C. Lee. Temperature solution of five-layer structure with an embedded circular source. In *Proceedings of the IEEE Intersociety Conference on Thermal Phenomena in Electronic Systems (I-THERM)*, 1992.

[6] J. Donald and M. Martonosi. Temperature-aware design issues for SMT and CMP architectures. In *Workshop on Complexity-Effective Design*, 2004.

[7] J.-M. Dorkel, P. Tounsi, and P. Leturcq. Three-dimensional thermal modeling based on the two-port network theory for hybrid or monolithic integrated power circuits. *IEEE Transactions on Components, Packaging, and Manufacturing Technology*, 19(4):501–507, December 1996.

[8] J. Clabes et al. Design and implementation of the POWER5 microprocessor. In *Proceedings of the 41st Design Automation Conference*, 2004.

[9] V. Gektin, R. Zhang, M. Vogel, G. Xu, and M. Lee. Substantiation of numerical analysis methodology for CPU package with non-uniform heat dissipation and heat sink with simplified fin modeling. In *Proceedings of the 9th Intersociety Thermal Phenomena (ITherm) Conference*, 2004.

[10] S.H. Gunther, F. Binns, D.M. Carmean, and J.C. Hall. Managing the impact of increasing microprocessor power consumption. *Intel Technology Journal*, (Q1), February 2001.

[11] S. Heo, K. Barr, and K. Asanović. Reducing power density through activity migration. In *Proceedings of the International Symposium on Low Power Electronics and Design*, 2003.

[12] Intel. Intel Pentium 4 processor on 90nm process thermal and mechanical design guidelines. Document 300564, February 2004.

[13] A.G. Kokkas. Thermal analysis of multiple-layer structures. *IEEE Transactions on Electron Devices*, ED-21(11):674–681, November 1974.

[14] B.S. Lall, B.M. Guenin, and R.J. Molnar. Methodology for thermal evaluation of multichip modules. *IEEE Transactions on Components, Packaging and Manufacturing Technology*, 18(4):758–764, December 1995.

[15] P. Leturcq, J.-M. Dorkel, A. Napieralski, and E. Lachiver. A new approach to thermal analysis of power devices. *IEEE Transactions on Electron Devices*, ED-34(5):1147–1156, May 1987.

[16] Y. Li, D. Brooks, Z. Hu, and K. Skadron. Performance, energy and thermal considerations for SMT and CMP architectures. In *Proceedings of the 11th International Symposium on High-Performance Computer Architecture*, 2005.

[17] C.H. Lim, W.R. Daasch, and G. Cai. A thermal-aware superscalar microprocessor. In *Proceedings of the International Symposium on Quality Electronic Design*, 2002.

[18] D. Maillet, S. André, J.C. Batsale, A. Degiovanni, and C. Moyne. *Thermal quadrupoles - Solving the heat equation through integral transforms.* Wiley, 2000.

[19] Y.J. Min, A.L. Palisoc, and C.C. Lee. Transient thermal study of semiconductor devices. In *Proceedings of the 6th SEMI-THERM Symposium*, 1990.

[20] A.V. Oppenheim, A.S. Willsky, and S.H. Nawab. *Signals and systems.* Prentice Hall, 1996.

[21] M.N. Özişik. *Boundary value problems of heat conduction.* Dover, 1968.

[22] C. Poirier, R. McGowen, C. Bostak, and S. Naffziger. Power and temperature control on a 90nm Itanium-family processor. In *Proceedings of the IEEE International Solid-State Circuits Conference*, 2005.

[23] M.D. Powell, M. Gomaa, and T.N. Vijaykumar. Heat-and-run: leveraging SMT and CMP to manage power density through the operating system. In *Proceedings of the 11th International Conference on Architectural Support for Programming Languages and Operating Systems*, 2004.

[24] N. Rinaldi. On the modeling of the transient thermal behavior of semiconductor devices. *IEEE Transactions on Electron Devices*, 48(12):2796–2802, December 2001.

[25] N. Rinaldi. Generalized image method with application to the thermal modeling of power devices and circuits. *IEEE Transactions on Electron Devices*, 49(4):679–686, April 2002.

[26] L. Shang, L.-S. Peh, A. Kumar, and N.K. Jha. Thermal modeling, characterization and management of on-chip networks. In *Proceedings of the 37th International Symposium on Microarchitecture*, 2004.

[27] K. Skadron, M.R. Stan, W. Huang, S. Velusamy, K. Sankaranarayanan, and D. Tarjan. Temperature-aware microarchitecture. In *Proceedings of the 30th Annual International Symposium on Computer Architecture*, 2003.

[28] H. Stehfest. Algorithm 368 : numerical inversion of Laplace transforms. *Communications of the ACM*, 13(1), January 1970. Erratum: remark on algorithm 368, vol. 10, No. 13, Oct. 1970.

[29] G. Xu, B. Guenin, and M. Vogel. Extension of air cooling for high power processors. In *Proceedings of the 9th Intersociety Thermal Phenomena (ITherm) Conference*, 2004.

Unité de recherche INRIA Lorraine, Technopôle de Nancy-Brabois, Campus scientifique,
615 rue du Jardin Botanique, BP 101, 54600 VILLERS LÈS NANCY
Unité de recherche INRIA Rennes, Irisa, Campus universitaire de Beaulieu, 35042 RENNES Cedex
Unité de recherche INRIA Rhône-Alpes, 655, avenue de l'Europe, 38330 MONTBONNOT ST MARTIN
Unité de recherche INRIA Rocquencourt, Domaine de Voluceau, Rocquencourt, BP 105, 78153 LE CHESNAY Cedex
Unité de recherche INRIA Sophia-Antipolis, 2004 route des Lucioles, BP 93, 06902 SOPHIA-ANTIPOLIS Cedex

Éditeur
INRIA, Domaine de Voluceau, Rocquencourt, BP 105, 78153 LE CHESNAY Cedex (France)
http://www.inria.fr
ISSN 0249-6399